

---

01 Apr 2017

## Field-Scale Observations of a Transient Geobattery Resulting from Natural Attenuation of a Crude Oil Spill

Jeffrey W. Heenan

Dimitrios Ntarlagiannis

Lee D. Slater

Carol L. Beaver

*et. al.* For a complete list of authors, see [https://scholarsmine.mst.edu/geosci\\_geo\\_peteng\\_facwork/1289](https://scholarsmine.mst.edu/geosci_geo_peteng_facwork/1289)

Follow this and additional works at: [https://scholarsmine.mst.edu/geosci\\_geo\\_peteng\\_facwork](https://scholarsmine.mst.edu/geosci_geo_peteng_facwork)

 Part of the [Geology Commons](#)

---

### Recommended Citation

J. W. Heenan et al., "Field-Scale Observations of a Transient Geobattery Resulting from Natural Attenuation of a Crude Oil Spill," *Journal of Geophysical Research: Biogeosciences*, vol. 122, no. 4, pp. 918-929, American Geophysical Union (AGU), Apr 2017.

The definitive version is available at <https://doi.org/10.1002/2016JG003596>

This Article - Journal is brought to you for free and open access by Scholars' Mine. It has been accepted for inclusion in Geosciences and Geological and Petroleum Engineering Faculty Research & Creative Works by an authorized administrator of Scholars' Mine. This work is protected by U. S. Copyright Law. Unauthorized use including reproduction for redistribution requires the permission of the copyright holder. For more information, please contact [scholarsmine@mst.edu](mailto:scholarsmine@mst.edu).

## RESEARCH ARTICLE

10.1002/2016JG003596

## Key Point:

- This study shows evidence of a biogeobattery observed in the field

## Correspondence to:

J. W. Heenan,  
jheenan@scarletmail.rutgers.edu

## Citation:

Heenan, J. W., D. Ntarlagiannis, L. D. Slater, C. L. Beaver, S. Rossbach, A. Revil, E. A. Atekwana, and B. Bekins (2017), Field-scale observations of a transient geobattery resulting from natural attenuation of a crude oil spill, *J. Geophys. Res. Biogeosci.*, 122, 918–929, doi:10.1002/2016JG003596.

Received 21 AUG 2016

Accepted 2 APR 2017

Accepted article online 6 APR 2017

Published online 24 APR 2017

## Field-scale observations of a transient geobattery resulting from natural attenuation of a crude oil spill

J. W. Heenan<sup>1</sup> , D. Ntarlagiannis<sup>1</sup>, L. D. Slater<sup>1</sup> , C. L. Beaver<sup>2</sup> , S. Rossbach<sup>2</sup>, A. Revil<sup>3</sup>, E. A. Atekwana<sup>4</sup> , and B. Bekins<sup>5</sup> 

<sup>1</sup>Department of Earth and Environmental Sciences, Rutgers University-Newark Campus, Newark, New Jersey, USA,

<sup>2</sup>Department of Biological Sciences, Western Michigan University, Kalamazoo, Michigan, USA, <sup>3</sup>ISTerre, CNRS, UMR CNRS

5275, Université de Savoie Mont-Blanc, Le Bourget-du-Lac, France, <sup>4</sup>Boone Pickens School of Geology, Oklahoma State

University, Stillwater, Oklahoma, USA, <sup>5</sup>United States Geological Survey (USGS), Menlo Park, California, USA

**Abstract** We present evidence of a geobattery associated with microbial degradation of a mature crude oil spill. Self-potential measurements were collected using a vertical array of nonpolarizing electrodes, starting at the land surface and passing through the smear zone where seasonal water table fluctuations have resulted in the coating of hydrocarbons on the aquifer solids. These passive electrical potential measurements exhibit a dipolar pattern associated with a current source. The anodic and cathodic reactions of this natural battery occur below and above the smear zone, respectively. The smear zone is characterized by high magnetic susceptibility values associated with the precipitation of semiconductive magnetic iron phase minerals as a by-product of biodegradation, facilitating electron transfer between the anode and the cathode. This geobattery response appears to have a transient nature, changing on a monthly scale, probably resulting from chemical and physical changes in subsurface conditions such as water table fluctuations.

### 1. Introduction

A “geobattery” describes the occurrence of a natural source of current flow inside a metallic conductor buried in the ground. This source of current is driven by a difference of redox potential in the ground and the two electrochemical half-cell reactions occurring simultaneously at separate locations on an ore body [Sato and Mooney, 1960; Bigalke and Grabner, 1997]. The current flow resulting from the half-cell reactions can be inferred using the self-potential (SP) method. This method is a passive electrical geophysical method used to map the occurrence of electrical potential anomalies occurring at the surface of the Earth. The term “biogeobattery” has since been adopted to describe SP anomalies associated with two electrochemical half-cell reactions occurring at separate locations, with different redox states electronically connected and being the result of microbial processes [Naudet et al., 2003; Naudet and Revil, 2005]. Conceptually, a biogeobattery results from a strong redox potential gradient in which the electron transfer between the anodic and cathodic reaction is driven by biotic electronic conductors such as certain pili between bacteria or certain filamentous (cable) bacteria [Naudet and Revil, 2005; Revil et al., 2010; Risgaard-Petersen et al., 2014]. Naudet and Revil [2005] suggested a biogeobattery can be generated by the oxidation of organic matter, in which the anaerobic oxidation occurs below the water table in an anoxic environment and the oxygen above the water table serves as the terminal electron acceptor. Since then, several additional electrochemical half-cell reactions have been proposed that could also support anode to cathode electron transfer [Revil et al., 2010], suggesting that a biogeobattery can develop in the presence of any redox gradient, not requiring oxygen as the electron acceptor. For example, Risgaard-Petersen et al. [2014] presented a biogeobattery in marine sediments with supporting evidence that certain oxidized nitrogen species are capable of acting as a terminal electron acceptor for the cathode portion of the geobattery.

The first evidence for the creation of such a biogeobattery at the field scale has been documented in a surface SP survey over the Entressen landfill in France [Naudet et al., 2004; Revil et al., 2010]. Additionally, Revil et al. [2010] presented surface SP data sets over two additional contaminated sites that were consistent with the operation of a geobattery. Risgaard-Petersen et al. [2014] presented evidence of current production in a marine biogeobattery setting, consistent with the modeled current production at the Entressen landfill [Linde and Revil, 2007]. Laboratory investigations attempted to shed more light into the biogeobattery mechanism. Naudet and Revil [2005] reported SP signals in an experimental tank treated with sulfate-reducing bacteria

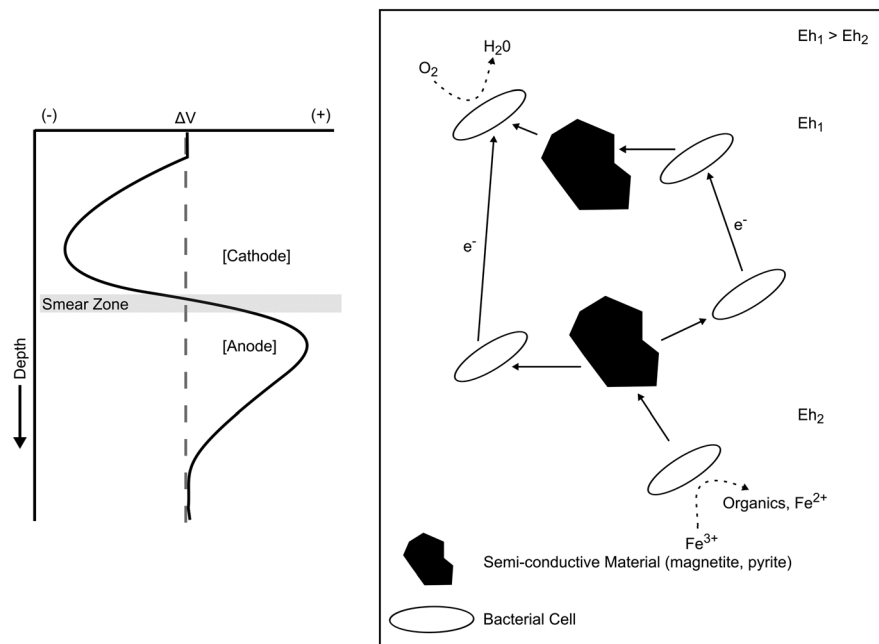


**Figure 1.** Conceptual model of the electron flow pathway potentially explaining the results seen during the duration of the experiment. In this model, multiple redox couples transfer electrons from deeper in the subsurface, below the water table, to the shallow subsurface above the water table. This transfer is facilitated by magnetite formed as a by-product of natural attenuation of the hydrocarbons in the contaminated zone. This results in the biogeobattery measured at the site (modified from *Revil et al.* [2010]).

and organic nutrients that are consistent with the geobattery concept. *Ntarlagiannis et al.* [2007] presented a column experiment in which the essential elements of a biogeobattery were produced, including geopili linking cells to cells and cells to mineral surfaces as confirmed by scanning electron microscope imaging. Electrical potential measurements on the scale of tens of millivolts were observed during this experiment. The sources of these potentials, however, were not conclusively produced by a geobattery. They could have possibly been the result of open circuit galvanic cell potentials facilitated by the metallic surfaces of the electrodes measuring electrical potential being in contact with the pore fluids. In another experiment, *Hubbard et al.* [2011] presented a column experiment where an oxic zone transitioned into an anoxic Fe(III)-reducing section mediated by a natural microbial community or a model iron-reducing organism, but no SP signal was recorded from this experiment. *Davis et al.* [2010] also only observed a small SP signal, typically  $<10$  mV, when injecting contaminated material into a biological permeable reactive barrier. The measured signal was deemed too small to be accurately and reliably measured in the field. The difficulty in monitoring these biogeobattery reactions in situ may result from the difficulties in recreating the complex biological environment and processes rather than deficiencies in the SP method. For example, *Revil et al.* [2015] simulated geobattery operation with a sandbox experiment in which an iron bar facilitated electron flow from a propylene glycol media below the water table to the oxygen electron acceptor in the unsaturated region and successfully monitored current flow.

*Revil et al.* [2010] emphasized that the key diagnostic factor when determining the presence of a biogeobattery generated by a biodegrading contaminant is a vertically oriented dipole, pointed upward, straddling a contaminant plume located at the water table (Figure 1), a phenomenon that has been observed in the field [*Doherty et al.*, 2015]. *Revil et al.* [2010] presented a laboratory experiment in which a bacteria-inoculated sandbox and mineral oil generated a small dipolar anomaly across the water table consistent with the biogeobattery model.

Vertical (downhole) SP profiles could confirm the operation of a biogeobattery at a contaminated site, as measurements of the electrical potential across the biodegrading contaminant from cathode to anode can be collected this way. Here we report results of a focused field investigation where such a data set was acquired over a mature hydrocarbon-contaminated site at the Bemidji, Minnesota, USA oil spill site. Our



**Figure 2.** Aerial map of the site indicating pool locations. This site was chosen for its thorough characterization and relatively well-controlled site conditions.

study focused on the North Pool (Figure 2) where oil floating at the water table is thickest and previous investigations provide an extensive geochemical inventory. The smear zone is a region in which the hydrocarbons are coating solids within the subsurface, the boundaries of which are defined by the range of water table fluctuations [Essaid *et al.*, 2011]. Also, it is microbially very active and shows distinctively elevated and localized presence of conductive magnetite [Atekwana *et al.*, 2014]. SP anomalies recorded on the site suggest that SP signals can be generated due to biodegradation processes in hydrocarbon-contaminated sites that can be described by the operation of a biogebattery.

### 1.1. Field Site

In August 1979, a high-pressure crude oil pipeline ruptured, spilling roughly 1,700,000 L of crude oil in an uninhabited area near Bemidji, Minnesota, USA. Oil pooled in low-lying areas and sprayed over an area of 6500 m<sup>2</sup> southwest of the pipeline, forming the south and north contaminated zones, or pools (Figure 2). Following cleanup procedures, approximately 400,000 L of product still remained and percolated downward toward the water table, forming a perched oil layer approximately 1 m thick [Bennett *et al.*, 1993; Hult, 1984]. The site eventually became the National Crude Oil Spill Fate and Natural Attenuation Research Site (referred to from here on as the Bemidji site) a well-constrained field laboratory for studying biodegradation processes. The oil plume settled at the water table and has since reached a stable state, though fluctuations in the water table level have resulted in a smear zone centered on the mean water table level. This site is ideally suited for investigating evidence for a biogebattery as (1) it is a mature, stable spill site with extensively documented natural attenuation [Baedecker *et al.*, 1993; Essaid *et al.*, 2011] and (2) the lithology is relatively simple, consisting of ~20 m thick moderately calcareous sand and glacial outwash deposits overlying clayey till of unknown thickness [Bennett *et al.*, 1993]. In addition to the well-characterized subsurface lithology, the site's temperature, water level, and oil thickness are regularly monitored at dozens of places across the site.

Iron minerals, within the sands and glacial deposits, include goethite, hematite, magnetite, ferrihydrite, clinocllore, epidote, and possibly maghemite [Zachara *et al.*, 2004]. The smear zone appears to be dominated by magnetite [Atekwana *et al.*, 2014], due to the high magnetic susceptibility (MS) values observed [Mewafy *et al.*, 2011]. It is assumed that magnetite is dominating the MS response as magnetite production has been shown to result from both hydrocarbon biodegradation [McCabe *et al.*, 1987] and dissimilatory iron reduction [Lovley *et al.*, 1987]. The uncontaminated groundwater is aerobic with dissolved oxygen concentrations between 8 and 9 mg/L, dissolved organic carbon of 2.8 mg/L, and low levels of nitrate at generally <0.2 mg/L, and sulfate at 2.9 mg/L [Bennett *et al.*, 1993]. The aquifer is divided in the vicinity of the oil body into anoxic, transition, and background zones. In the anoxic portion, hydrocarbons are oxidized

predominantly by iron reduction [Lovley *et al.*, 1989] and methanogenesis [e.g., Baedecker *et al.*, 1993]. Bekins *et al.* [2001] show two zones of methanogenic activity with CH<sub>4</sub> concentrations greater than 15 mg/L. The vadose zone vapor plume near the oil body has low O<sub>2</sub> (< 2% of volume), high CO<sub>2</sub> (>10%), and high CH<sub>4</sub> (>15%) levels [Amos *et al.*, 2005]. This site has been extensively documented in other research [e.g., Essaid *et al.*, 2011].

## 2. Methods

### 2.1. Self-Potential

In June 2010, an ~5 cm diameter borehole (C1010) was drilled at a site on the North Pool where extensive microbiological [Bekins *et al.*, 2001; Beaver *et al.*, 2015] and geochemical [Cozzarelli *et al.*, 2010] studies have been conducted (Figure 2). The borehole was drilled by advancing a core barrel with a polycarbonate liner ahead of a hollow stem auger to ~15 m below land surface, and ~6 m below the mean water table elevation. An array of 16 nonpolarizing Petiau Pb-PbCl electrodes [Petiau, 2000] was assembled by attaching the electrodes to a 3.8 cm diameter PVC pipe, with connecting wires extending along the pipe to the surface. Electrodes were spaced at 1 m intervals, starting at 1 m below land surface (BLS), and straddling the smear zone. An additional electrode was placed at 7.5 m BLS to focus on the smear zone. The array was installed in the borehole immediately after drilling, and the borehole backfilled using a slurry of the native material produced during drilling. SP signals were recorded using a high impedance voltmeter (100 MΩ) with the uppermost electrode assigned as the reference electrode, which was connected to the negative terminal of the voltmeter by convention. Water and oil levels also were collected each month in an adjacent well located less than a meter from the electrode array.

### 2.2. Magnetic Susceptibility

In June 2011, magnetic susceptibility (MS) logging measurements were acquired in an existing well (G0906) located approximately 8 m from C1010. Data were acquired at 3 cm intervals from land surface to 17 m below land surface using a Bartington MS logging probe calibrated for a PVC lined well with an ~5 cm diameter. Additionally, the retrieved cores were logged in the laboratory. An example of the methods and results were previously reported in detail in Mewafy *et al.* [2011].

### 2.3. Microbiology

Samples for DNA extraction were obtained from core C1110, which was retrieved from the smear zone in June 2011 close to C1010. The retrieved core, consisting of 14 sections, started at an elevation of 432.0 m above sea level (asl) and spanned a distance of 10.67 m to the region below the surface of the water table. Sediment cores were retrieved in polycarbonate liners in a core barrel pushed into the sediments ahead of a hollow stem auger. Liquid CO<sub>2</sub> injected into the shaft of a freezing drive shoe in the last 10 cm of the saturated zone core froze the water allowing for retention of water throughout the core [Murphy and Herkelrath, 1996]. The cores were frozen, sealed, and transported to Oklahoma State University for analysis. A sterile spatula was used to extract the sediments, and the sediment samples were placed aseptically into 1.7 mL microcentrifuge tubes. Twelve samples were taken along the core in triplicates. The sediment samples were stored at –20°C in order to preserve the DNA until extraction. The PowerSoil DNA Isolation Kit (MOBIO Laboratories, Carlsbad, CA) was used to isolate soil DNA. Isolated DNA was stored at –20°C. In this work, the microbial abundance of three samples in the relevant zone (423.6, 424.1, and 425.1 m asl) is shown.

Extracted DNA was sent to the Michigan State University Genomics Core Facility for 16S rRNA gene high-throughput sequencing using primers F515 and R806 with the Illumina MiSeq platform. Paired end sequences were assembled with PANDAseq [Masella *et al.*, 2012], resulting in a total of 1,764,706 sequences. Sequences that did not overlap by 10 base pairs, were shorter than 250 bp, longer than 274 bp or did not meet a quality score or 0.9, were removed. OTUs were picked by the pick\_open\_reference\_otus.py command using usearch61 [Edgar, 2010] in QIIME [Caporaso *et al.*, 2010]. Singletons were removed, and taxonomy was assigned by using the default QIIME Greengenes reference data set. Sequences were deposited in the National Center for Biotechnology Information Sequence Read Archive under the submission number SUB2352145.



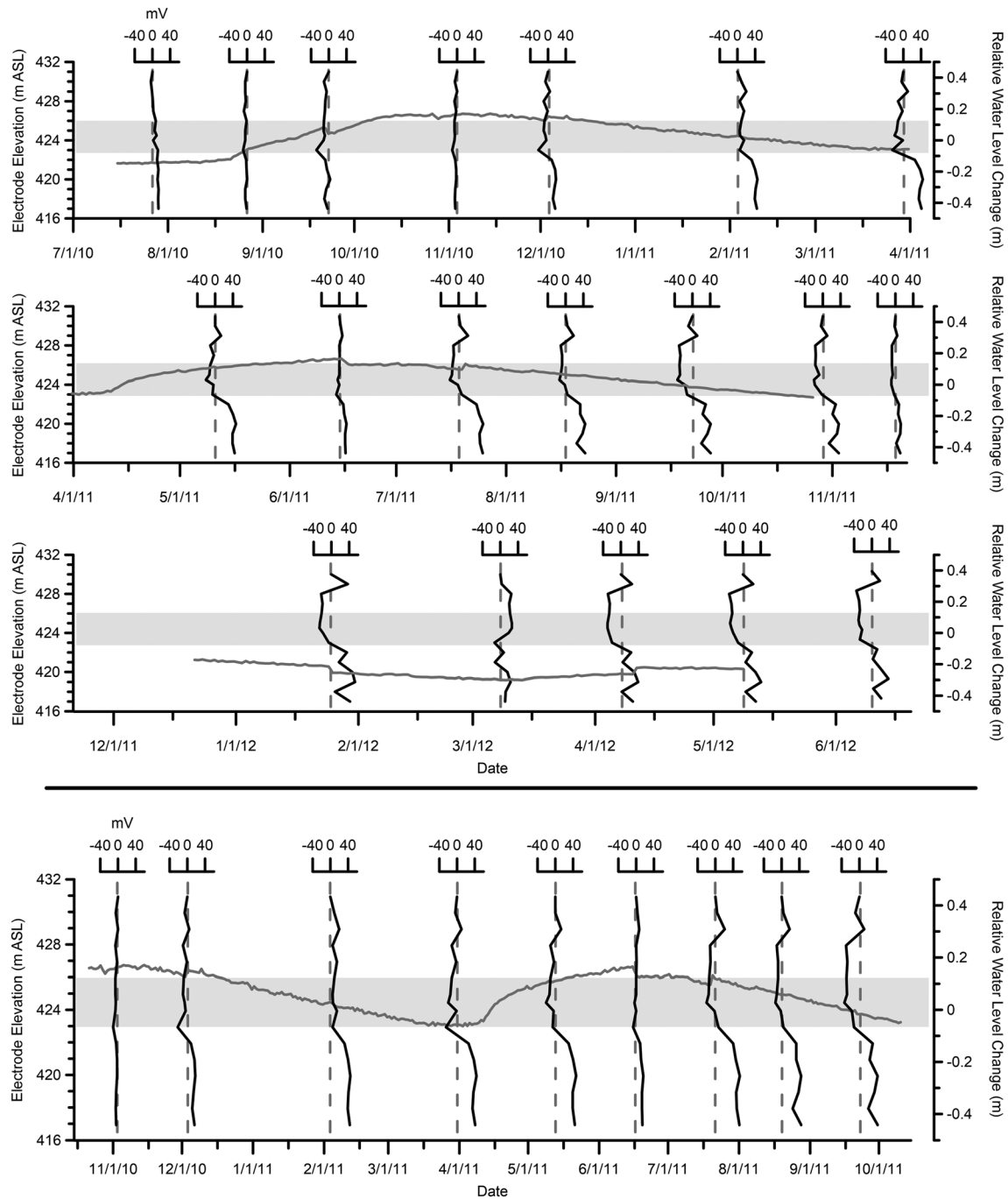


**Figure 3.** (top) Time series of the SP data collected from July 2010 to July 2012. Measurements in early-November 2010 show no indication of the strong dipole seen in the subsequent measurements from December 2010 to June 2011. The dipole decreases in the mid-June 2011 measurements and subsequently increases in the measurements following this data set. The smear zone is indicated by the shaded rectangle and a vertically exaggerated plot of the relative water level change is represented by the gray line. (bottom) A representative subset of the data with continuous water level monitoring suggests a link between the water level and the measured geobattery response.

### 3. Results

#### 3.1. Self-Potential

A time series of SP measurements for the duration of the experiment is presented in Figure 3. This data set excludes the initial measurements, as there appears to be have been a period of time where the system

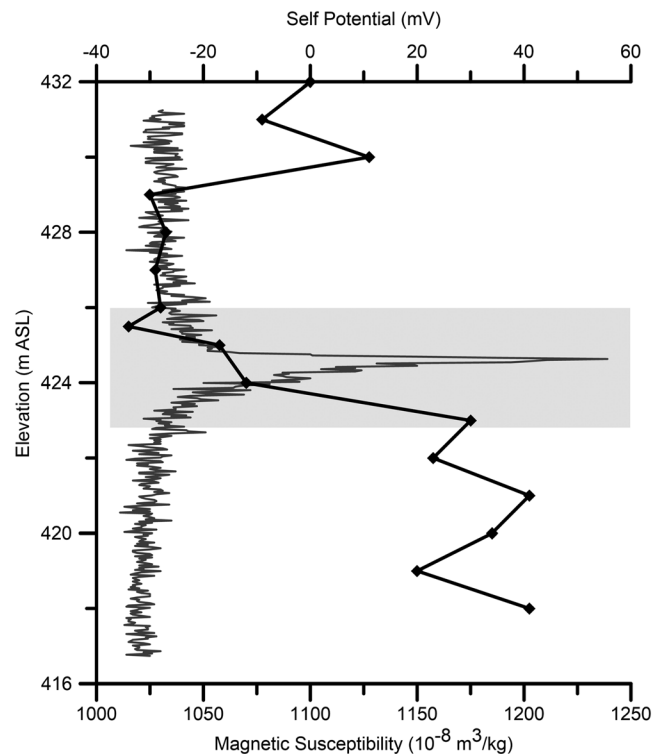


**Figure 4.** The dipolar SP anomaly observed at this site appears to be centered around the zone of highest MS. The MS data are represented by the gray line, a representative SP profile by the black line/diamonds, and smear zone is represented by the light gray shaded area.

seems to become stronger with time. The water level data presented in the figure is from a level logger in an adjacent well.

### 3.2. Magnetic Susceptibility

Magnetic susceptibility measurements performed down borehole G0906, less than 6 m north of borehole C1010, reveal a strong MS signal within the smear zone (Figure 4). Whereas most of the borehole shows a MS of  $1020 \pm 15 \text{ m}^3/\text{kg}$  [Atekwana *et al.*, 2014], there is a sharp increase in MS to maximum values of  $1230 \text{ m}^3/\text{kg}$  in the smear zone; even with the elevated MS values recorded in the borehole, the local spike around the smear zone is very distinctive (Figure 4). The MS signal and the dipolar SP signature are centered on the smear zone (Figure 4). Analysis of the sediment reveals that the horizon of high magnetic susceptibility coincides with a zone of high magnetite content [Mewafy *et al.*, 2011; Atekwana *et al.*, 2014]. The magnetic susceptibility and sediment analysis of the site is further documented in Atekwana *et al.* [2014].

### 3.3. Microbiology

Because of hydrocarbon degradation processes, the oil plume and the smear zone above are an area of intense microbial activity. At 425.1 m (above sea level; m asl), which is in the smear zone above the oil plume, the *Peptococcaceae* family predominated, making up 27% of the total microbial community, followed by the *Comamonadaceae* with 18%. The main genus among the *Peptococcaceae* was closely related to WCHB1-84, an iron-reducing Gram-positive bacterium, the sequence of which was originally found at the contaminated Wurtsmith air force base [Dojka *et al.*, 1998]. The main genus among the *Comamonadaceae* was *Albidiferax* (*Rhodoferax*), which is also a known iron reducer [Risso *et al.*, 2009]. The family of *Bradyrhizobiaceae* was found to be present with 4% abundance. The main representative of this family was *Rhodopseudomonas*, which is capable of iron oxidation and of accepting electrons in microbial fuel cells [Jiao *et al.*, 2005; Xing *et al.*, 2008]. At the two lower depths, at 424.1 and 423.6 m, which are inside the oil plume, a clearly methanogenic microbial community was present predominated by the *Syntrophaceae* with 40% and 32%, respectively, and the methanogenic *Methanoregulaceae* with 15% and 11%, respectively. The main genus among the

was stabilizing or reaching equilibrium. Continuous water level monitoring data for this time period are also shown on the lowest panel. The first set of measurements, taken on 3 November 2010 after an apparent equilibrium was reached, shows no evidence of a diagnostic dipole typical of a geobattery. The subsequent measurements from December 2010 to June 2011 show the dipole signature, which appears to increase in magnitude with time subsequently decreasing for the mid-June 2011 measurement. The dipole is characterized by negative values above the smear zone, and positive values at the bottom consistent with the suggested biogeobattery model [Revil *et al.*, 2010]; in all cases, the magnitude of the negative potential is smaller than that of the positive potential. The dipole then strengthens from mid-July to October, the end of the time window presented in Figure 3. Once again, this dipole

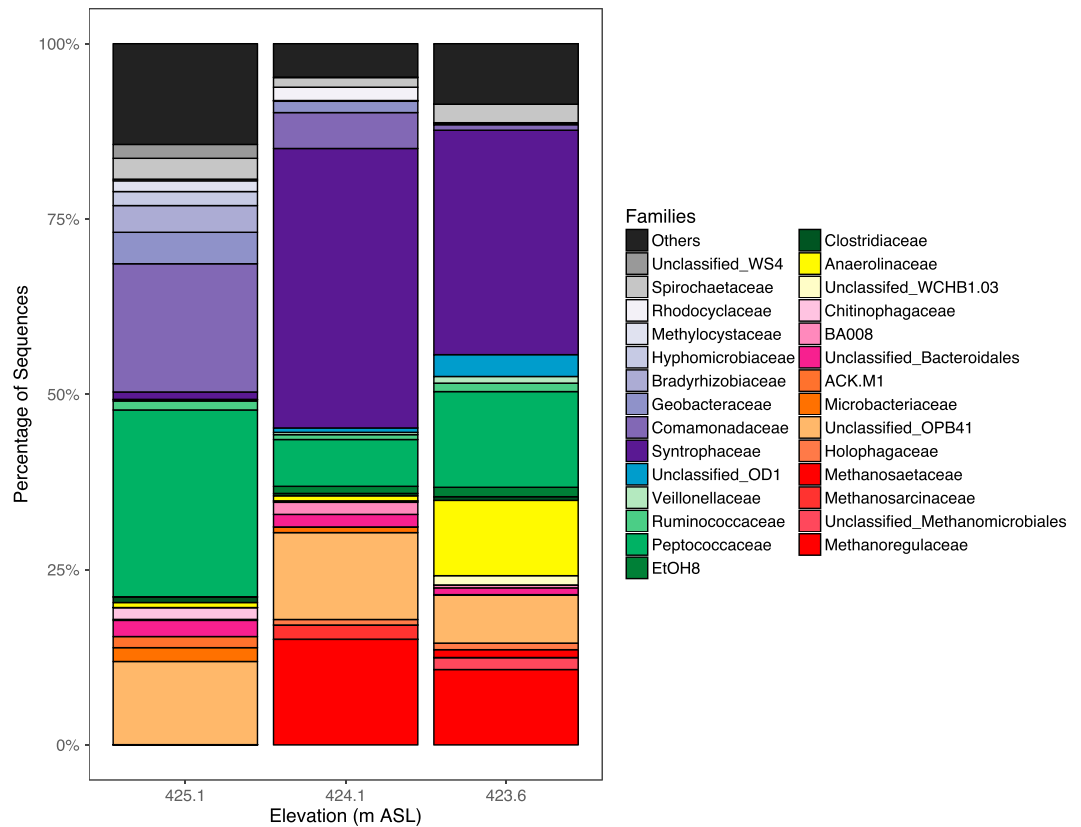


**Figure 5.** Microbial community structure in the center of petroleum contamination of the North Pool at Bemidji, MN in June 2011. Bacterial and archaeal 16S rRNA sequence abundances are sorted by families. The prominent microbial families in the smear zone at 425.1 m (above sea level, m asl) are the unclassified *Peptococcaceae* of the *Firmicutes* and the *Comamonadaceae* of the *Beta-Proteobacteria*. In the free phase zone at 424.1 and 423.6 m asl, the dominant families are *Syntrophaceae* of the *Delta-Proteobacteria* and the archaeal family *Methanoregulaceae*. “Others” denote microbial families that make up less than 1% of the total community.

*Syntrophaceae* was *Smithella*, which frequently has been reported to be associated with the methanogenic degradation of crude oil alkanes [Gray et al., 2011] (Figure 5).

#### 4. Discussion

We have reported the presence of a strong SP anomaly centered across the smear zone of a crude oil plume undergoing biodegradation (Figure 3). This smear zone is concomitant with the presence of strong values in the magnetic susceptibility (Figure 4). The SP anomaly is also transient with a loose relationship with seasonal fluctuations in water table elevations. These observations point to the existence of a possible biogeo-battery driven by microbially mediated redox reactions associated with the degradation of the crude oil. A biogeo-battery requires the presence of a strong redox gradient above and below the water table and an electronic conductor that bridges the two redox couples [Revil et al., 2010]. These conditions appear to be present at the Bemidji site. Our data suggest that the presence of magnetite may serve as the electronic conductor. Indeed, several studies have documented that magnetite can be used by microbes as conduit for direct interspecies electron transfer [Kato et al., 2012; Shrestha et al., 2013; Rotaru et al., 2014] and has been shown to accelerate syntrophic methanogenesis [Cruz Viggj et al., 2014; Zhuang et al., 2015].

Detailed microbial characterization of the Bemidji site indicate that syntrophic bacteria and methanogenic archaea are present in the oil plume and iron reducers are present in the smear zone above the methanogenic zone (Figure 5). Bacteria from the genus *Smithella* are able to provide hydrogen and carbon dioxide to methanogenic archaea and indeed, the main methanogen found at these depths in our study was *Methanoregula*, which is a hydrogenotrophic Archaeon. *Methanoregula* was shown to be enriched in



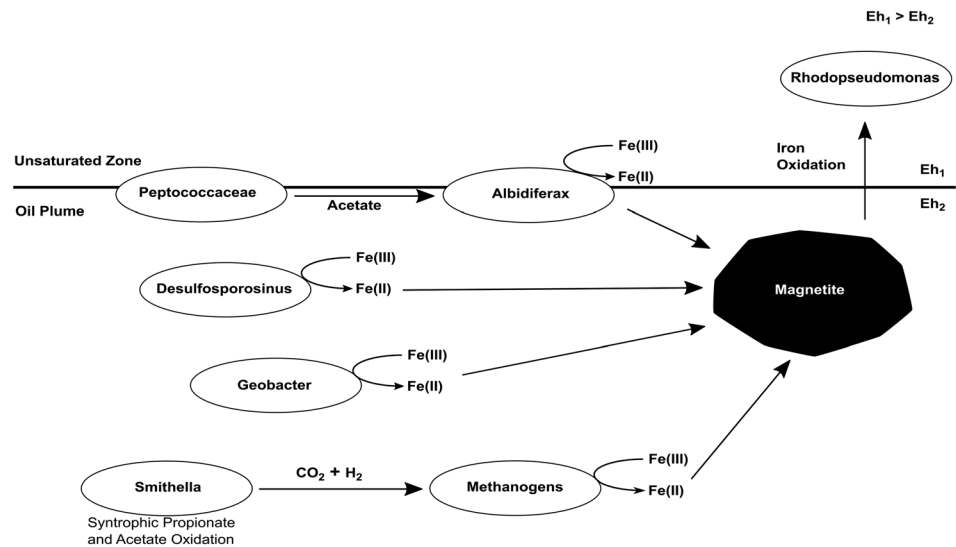


**Figure 6.** A flow diagram of the interspecies interactions between the microbes in the subsurface that result in the biogeobattery measured at the site. Iron-reducing and methanogenic microbes within the saturated smear zone generate magnetite which is subsequently oxidized in the unsaturated zone, resulting in the upward flow of electrons in the subsurface.

microcosms that were inoculated with lake sediments and incubated with butyrate and magnetite nanoparticles [Zhang and Yu, 2016]. It is assumed that *Methanoregula* is able to take up electrons directly from magnetite, because in another study, *Methanoregula* was found to be enriched at cathodes and producing methane, when the voltage was set lower than the threshold for hydrogen production [Chen et al., 2016]. The presence of the electron conductor magnetite or a combination of magnetite and microbial influences (biofilms, nanowires, etc.), has been verified by the MS field measurements and laboratory analysis of retrieved sediments of the smear zone.

The observed SP dipole, with negative anomalies above the smear zone, and positive below, is consistent with a bulk upward flow of electrons from below the saturated zone into the unsaturated zone. Excess of electrons below the smear zone can be explained by the dominant reducing conditions (methanogenesis). In a similar fashion, electron depletion above the smear zone can be the result of iron reduction, even coupled to iron oxidation as suggested by the presence of *Rhodopseudomonas* higher up. In this environment, biogenic magnetite formation may be encouraged by methanogenic/iron reduction processes. The presence of magnetite, and/or the electrically conductive biofilms, will promote upward flow of electrons, and its subsequent oxidation by *Rhodopseudomonas* in the region above the water table. Analyzing these metabolic pathways as a complementary system, where both regions work in unison, electron flow can be traced from the methanogenic zone below the water table to the zone above (Figure 6). This microbially driven flow of electrons across the conductive boundary can result in the dipolar anomaly, interpreted as the biogeobattery. The following equations describe possible redox processes that could drive the biogeobattery and are supported by the microbiology:



The vertical SP anomaly observed suggests that the plume fringe concept [Meckenstock et al., 2015] may best describe redox zonation at the site. In this model, the metabolic processes of natural attenuation take place simultaneously on the fringes of the plume, with multiple processes occurring on the same horizon (Figure 7).

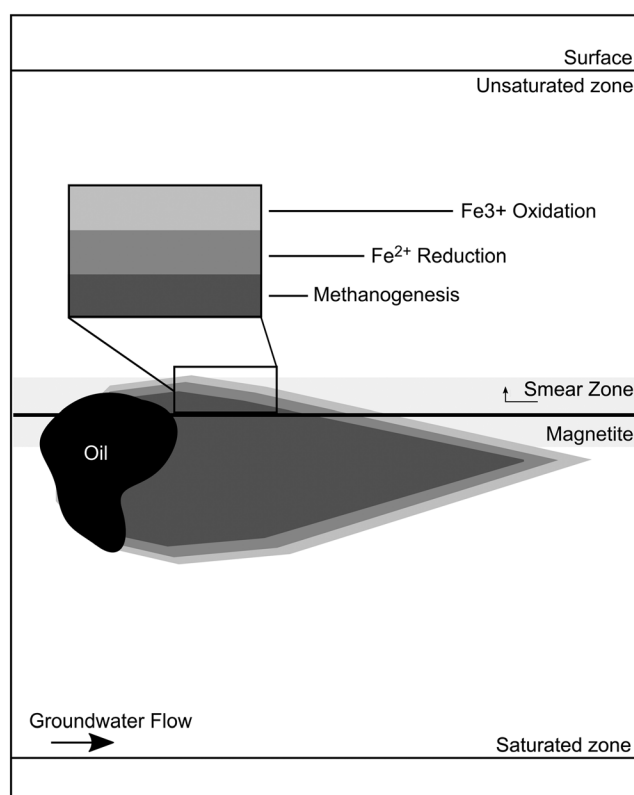


**Figure 7.** Conceptual model of plume fringe degradation [Meckenstock *et al.*, 2015]. This model supports a vertical gradient in redox potential rather than a horizontal gradient dependent on the direction of groundwater flow.

[Lovley *et al.*, 1987; Finneran *et al.*, 2003; Hansel *et al.*, 2005], thereby providing an electron conductor to facilitate electron flow. Magnetite can be used by microbes as conduit for direct interspecies electron transfer [Kato *et al.*, 2012; Shrestha *et al.*, 2013; Rotaru *et al.*, 2014] and has been shown to accelerate syntrophic methanogenesis [Cruz Viggi *et al.*, 2014; Zhuang *et al.*, 2015]. Additionally, iron-oxidizing microbial genera, such as *Rhodospseudomonas*, [Xing *et al.*, 2008; Bose *et al.*, 2014; Cruz Viggi *et al.*, 2014] are shown to be present above the anoxic zone in this work. This may result in the redox gradient required to generate the geobattery.

The complex microbial community below the smear zone appears to be a contributing factor to the transience of the biogeobattery. As evidenced by the diverse microbial families present, there are diverse metabolic pathways, including those for iron reduction and methanogenesis. The presence of diverse microbial populations suggests dynamic geochemical conditions that could favor certain populations in response to changes in local environmental conditions (e.g., water level). Changes in the dominance of certain metabolic pathways could explain the transient nature of SP and MS signals at the Bemidji site [Slater *et al.*, 2015]. Such a dynamic environment is in agreement with the fringe plume concept, where the redox gradients are very closely spaced at the outer edge of the plume (Figure 7) [Meckenstock *et al.*, 2015]—exactly like the conditions at the Bemidji site. As previously discussed, the biogeobattery operation requires a redox gradient across the electron conductor (in agreement with the fringe plume concept) and not necessary an oxic/anoxic boundary as previously thought [Revil *et al.*, 2010]. While metatranscriptomics could have provided a clearer picture as to what metabolic pathways were active at the time of sampling, we cannot verify if the presence of diverse microbial populations with the ability to express multiple metabolic pathways are the result of dynamic geochemical conditions (e.g., temperature and oxygen availability), or the drivers for such changes. However, the transient geophysical signals observed appear to be linked to dynamic microbial processes. Due to the lack of a temperature gradient and slow moving groundwater, this signal appears to be driven by the redox gradient [Essaid *et al.*, 2011]. As this gradient appears to be dynamic, we expect the SP signal to vary over time in response to these changes. This supports the concept that the SP signal as an indirect

This differs from the traditional zonal model, where different metabolic processes occur in different regions, typically in the direction of groundwater flow. Recent microbiological characterization of the site supports this model. Iron-reducing bacteria such as *Albidiferax* and *Desulfosporosinus* and two methanogenic archaea, *Methanoregula* and *Methanosarcina*, were identified in clone libraries constructed from DNA isolated from Bemidji sediments at the same depth [Beaver *et al.*, 2015], and with 16S rRNA gene sequencing in this work.

The geochemical and microbial characterization of the site suggests that the essential biogeobattery components are present and can be linked to the indigenous microbial community. In this publication, we include a more comprehensive microbiological analysis based on 16S rRNA gene high-throughput sequencing. For example, microbes were found that are capable of producing secondary magnetite due to iron reduction, including *Geobacter* and *Albidiferax*,

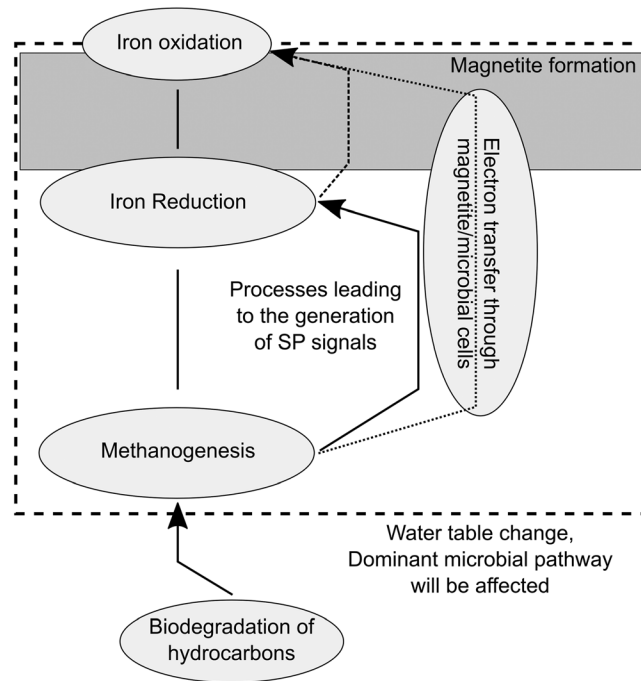


**Figure 8.** A concept map of the biogeobattery seen on the site. When the electrons are recycled back into the system, changes such as water table fluctuation may result in a change in the dominant microbial pathway, subduing the measured SP signal.

table elevation and the strength of the dipole as computed above. The linear correlation coefficient ( $R^2$ ) for the least squares regression of the geobattery strength as a function of the water table is 0.43, but it is significant ( $P = 0.011$ ) at the 95% confidence interval. The weak  $R^2$  value associated with the strength of the dipole and the water level is not necessarily indicative of these two variables being unrelated. The expected wetting/drainage hysteresis [Essaid et al., 2011] is complicated by oil in the pore space altering water flow during the rising and falling of the water table. Furthermore, nutrient recharge patterns may be influenced by these same factors, resulting in variations in biodegradation rates and microbial activity [Bekins et al., 2005]. Targeted experiments are required to fully understand the influence of the complex hysteresis patterns on the SP signal. The water level fluctuations might promote changes in the local redox conditions, leading to changes in the dominant microbial populations with different metabolic capabilities (Figure 8), further promoting redox changes; this sequence of events could be expressed as a transient biogeobattery. The weak correlation between the water table level and the dipole strength indicates that the relationship is more complex than that and that there could be several variables influencing this relationship.

The results of this study suggest that the observed SP signals are closely linked to microbial processes. Specifically, the complex geochemical environment supports the presence of diverse microbial populations with a multitude of metabolic pathways and can be linked with both the biodegradation processes and the SP signal. Variations in these pathways may drive the signal transience. This study demonstrates the current ability of SP to be used as a qualitative monitoring tool for natural attenuation. The influence of complex microbial environments demonstrates the need for further research to identify the signal sources. For example, iron recycling in magnetite by iron-metabolizing microorganisms may potentially drive geobattery operation [Byrne et al., 2015].

### 5. Conclusions

The SP data sets collected over the course of this field study indicate that a field-scale biogeobattery exists at the Bemidji site. This biogeobattery is transient, with periods of little to no measurable voltage signature across the smear zone of the hydrocarbon contamination, likely due to subsurface conditions. The driving

indicator of natural attenuation processes [Doherty et al., 2010, 2015]. Further research is needed to clarify which microbiological driven processes contribute to the biogeobattery operation, as evidenced in SP measurements, and which do not. Once the contributing processes have been verified, then quantitative interpretation of the SP signals may then be possible.

Further support for our conceptual model is the apparent correlation of the water table fluctuation with the observed SP dipole (Figure 3). Throughout the experiment, relative highs in the water table were followed by weak dipoles, while lower relative water table levels were followed by stronger dipoles. For example, Figure 3 shows that the water table recorded at an adjacent well is higher on 3 November 2010 and 15 June 2011 when the dipole is weak. There is a weak negative linear correlation between the water

force for this transient signal appears to be variations in the environment within and immediately adjacent to the plume. When considered in the context of the plume fringe concept [Meckenstock *et al.*, 2015], the bulk of the redox couples hypothesized in Figure 6 occur in a comparatively small portion of the contaminated region. This would result in any physical or chemical changes (i.e., fluctuating water table) altering dominant pathways, resulting in the transient nature observed.

As SP is a relatively low-cost approach to monitoring natural attenuation, the ability to sense degradation processes observed during this experiment supports its viability for use in similar environments. Further exploration into the sources of signals observed during this experiment may hold the key to using this method in a more quantitative capacity.

#### Acknowledgments

Funding for this project was provided by Enbridge Energy (Ltd.), the Minnesota Pollution Control Agency, the USGS Toxic Substances Hydrology Program, and U.S. EPA Student Services contract EP10D000488. We thank Isabelle Cozzarelli (USGS) for insightful discussions regarding redox processes at Bemidji. Andrew Berg (USGS), Melinda Erickson (USGS), Jared Trost (USGS), Magnus Skold (CSM), and Farag Mewafy (Oklahoma State University) provided project support. The self-potential data presented here are available through the Rutgers University Community Repository at <https://rucore.libraries.rutgers.edu/research/>.

#### References

- Amos, R. T., K. U. Mayer, B. A. Bekins, G. N. Delin, and R. L. Williams (2005), Use of dissolved and vapor-phase gases to investigate methanogenic degradation of petroleum hydrocarbon contamination in the subsurface, *Water Resour. Res.*, *41*, W02001, doi:10.1029/2004WR003433.
- Atekwana, E. A., F. M. Mewafy, G. Abdel Aal, D. D. Werkema, A. Revil, and L. D. Slater (2014), High-resolution magnetic susceptibility measurements for investigating magnetic mineral formation during microbial mediated iron reduction, *J. Geophys. Res. Biogeosci.*, *119*, 80–94, doi:10.1002/2013JG002414.
- Baedecker, M. J., I. M. Cozzarelli, R. P. Eganhouse, D. I. Siegel, and P. C. Bennett (1993), Crude oil in a shallow sand and gravel aquifer—III. Biogeochemical reactions and mass balance modeling in anoxic groundwater, *Appl. Geochem.*, *8*(6), 569–586, doi:10.1016/0883-2927(93)90014-8.
- Beaver, C. L., A. E. Williams, E. A. Atekwana, F. M. Mewafy, G. A. Aal, L. D. Slater, and S. Rossbach (2015), Microbial communities associated with zones of elevated magnetic susceptibility in hydrocarbon-contaminated sediments, *Geomicrobiol. J.*, doi:10.1080/01490451.2015.1049676.
- Bekins, B. A., I. M. Cozzarelli, E. M. Gody, E. Warren, H. I. Essaid, and M. E. Tuccillo (2001), Progression of natural attenuation processes at a crude oil spill site: II. Controls on spatial distribution of microbial populations, *J. Contam. Hydrol.*, *53*(3–4), 387–406, doi:10.1016/S0169-7722(01)00175-9.
- Bekins, B. A., F. D. Hostettler, W. N. Herkelrath, G. N. Delin, E. Warren, and H. I. Essaid (2005), Progression of methanogenic degradation of crude oil in the subsurface, *Environ. Geosci.*, *12*(2), 139–152, doi:10.1306/eg.11160404036.
- Bennett, P. C., D. E. Siegel, M. J. Baedecker, and H. M.F. (1993), Crude oil in a shallow sand and gravel aquifer—I. Hydrogeology and inorganic geochemistry, *Appl. Geochem.*, *8*(6), 529–549, doi:10.1016/0883-2927(93)90012-6.
- Bigalke, J., and E. W. Grabner (1997), The Geobattery model: A contribution to large scale electrochemistry, *Electrochim. Acta*, *42*(23–24), 3443–3452, doi:10.1016/S0013-4686(97)00053-4.
- Bose, A., E. J. Gardel, C. Vidoudez, E. A. Parra, and P. R. Girguis (2014), Electron uptake by iron-oxidizing phototrophic bacteria, *Nat. Commun.*, *5*, 3391, doi:10.1038/ncomms4391.
- Byrne, J. M., N. Klueglein, C. Pearce, K. M. Rosso, E. Appel, and A. Kappler (2015), Redox cycling of Fe(II) and Fe(III) in magnetite by Fe-metabolizing bacteria, *Science*, *347*(6229), 1473–1476, doi:10.1126/science.aaa4834.
- Caporaso, J. G., et al. (2010), QIIME allows analysis of high-throughput community sequencing data, *Nat. Methods*, *7*(5), 335–336.
- Chen, Y., B. Yu, C. Yin, C. Zhang, X. Dai, H. Yuan, and N. Zhu (2016), Biostimulation by direct voltage to enhance anaerobic digestion of waste activated sludge, *RSC Adv.*, *6*(2), 1581–1588, doi:10.1039/C5RA24134K.
- Cozzarelli, I. M., B. A. Bekins, R. P. Eganhouse, E. Warren, and H. I. Essaid (2010), In situ measurements of volatile aromatic hydrocarbon biodegradation rates in groundwater, *J. Contam. Hydrol.*, *111*(1–4), 48–64, doi:10.1016/j.jconhyd.2009.12.001.
- Cruz Viggli, C., S. Rossetti, S. Fazi, P. Paiano, M. Majone, and F. Aulenta (2014), Magnetite particles triggering a faster and more robust syntrophic pathway of methanogenic propionate degradation, *Environ. Sci. Technol.*, *48*(13), 7536–7543, doi:10.1021/es5016789.
- Davis, C. A., L. D. Slater, B. Kulesa, A. S. Ferguson, E. A. Atekwana, R. Doherty, and R. Kalin (2010), Self-potential signatures associated with an injection experiment at an in situ biological permeable reactive barrier, *Near Surf. Geophys.*, 541–551, doi:10.3997/1873-0604.2010034.
- Doherty, R., B. Kulesa, A. S. Ferguson, M. J. Larkin, L. A. Kulakov, and R. M. Kalin (2010), A microbial fuel cell in contaminated ground delineated by electrical self-potential and normalized induced polarization data, *J. Geophys. Res.*, *115*, G00G08, doi:10.1029/2009JG001131.
- Doherty, R., B. McPolin, B. Kulesa, A. Frau, A. Kulakova, C. C. R. Allen, and M. J. Larkin (2015), Microbial ecology and geoelectric responses across a groundwater plume, *Interpretation*, *3*(4), 1–13, doi:10.1190/INT-2015-0058.1.
- Dojka, M. A., P. Hugenholtz, S. K. Haack, and N. R. Pace (1998), Microbial diversity in a hydrocarbon- and chlorinated-solvent- contaminated aquifer undergoing intrinsic bioremediation, *Appl. Environ. Microbiol.*, *64*(10), 3869–3877.
- Edgar, R. C. (2010), Search and clustering orders of magnitude faster than BLAST, *Bioinformatics*, *26*(19), 2460–2461, doi:10.1093/bioinformatics/btq461.
- Essaid, H. I., B. A. Bekins, W. N. Herkelrath, and G. N. Delin (2011), Crude oil at the Bemidji site: 25 years of monitoring, modeling, and understanding, *Ground Water*, *49*(5), 706–726, doi:10.1111/j.1745-6584.2009.00654.x.
- Finneran, K. T., C. V. Johnsen, and D. R. Lovley (2003), *Rhodoferrax ferrireducens* sp. nov., a psychrotolerant, facultatively anaerobic bacterium that oxidizes acetate with the reduction of Fe(III), *Int. J. Syst. Evol. Microbiol.*, *53*(3), 669–673, doi:10.1099/ijs.0.02298-0.
- Gray, N. D., et al. (2011), The quantitative significance of Syntrophaceae and syntrophic partnerships in methanogenic degradation of crude oil alkanes, *Environ. Microbiol.*, *13*(11), 2957–2975, doi:10.1111/j.1462-2920.2011.02570.x.
- Hansel, C. M., S. G. Benner, and S. Fendorf (2005), Competing Fe (II)-induced mineralization pathways of ferrihydrite, *Environ. Sci. Technol.*, *39*(18), 7147–7153.
- Hubbard, C. G., L. J. West, K. Morris, B. Kulesa, D. Brookshaw, J. R. Lloyd, and S. Shaw (2011), In search of experimental evidence for the biogeobattery, *J. Geophys. Res.*, *116*, G04018, doi:10.1029/2011JG001713.
- Hult, M. F. (1984), Groundwater contamination by crude oil at the Bemidji, Minnesota, research site—An introduction, *Groundw. Contam. by crude oil Bemidji, Minnesota, Res. site, US Geol. Surv. Water Resour. Investig. Rep.*, pp. 84–4188.

- Jiao, Y., A. Kappler, L. R. Croal, and D. K. Newman (2005), Isolation and characterization of a genetically tractable photoautotrophic Fe(II)-oxidizing bacterium, *Rhodopseudomonas palustris* strain TIE-1, *Appl. Environ. Microbiol.*, *71*(8), 4487–4496, doi:10.1128/AEM.71.8.4487-4496.2005.
- Kato, S., K. Hashimoto, and K. Watanabe (2012), Microbial interspecies electron transfer via electric currents through conductive minerals, *Proc. Natl. Acad. Sci. U.S.A.*, *109*(25), 10,042–10,046, doi:10.1073/pnas.1117592109.
- Linde, N., and A. Revil (2007), Inverting self-potential data for redox potentials of contaminant plumes, *Geophys. Res. Lett.*, *34*, L14302, doi:10.1029/2007GL030084.
- Lovley, D. R., J. F. Stolz, G. L. Nord, and E. J. P. Phillips (1987), Anaerobic production of magnetite by a dissimilatory iron-reducing microorganism, *Nature*, *330*(6145), 252–254, doi:10.1038/330252a0.
- Lovley, D. R., M. J. Baedeker, D. J. Lonergan, I. M. Cozzarelli, E. J. P. Phillips, and D. I. Siegel (1989), Oxidation of aromatic contaminants coupled to microbial iron reduction, *Nature*, *339*, 297–300, doi:10.1038/339297a0.
- Masella, A. P., A. K. Bartram, J. M. Truszkowski, D. G. Brown, and J. D. Neufeld (2012), PANDAseq: Paired-end assembler for illumina sequences, *BMC Bioinfo.*, *13*(1), 1–7, doi:10.1186/1471-2105-13-31.
- McCabe, C., R. Sassen, and B. Saffer (1987), Occurrence of secondary magnetite within biodegraded oil, *Geology*, *15*(1), 7–10, doi:10.1130/0091-7613(1987)15<7:OOSMWB>2.0.CO;2.
- Meckenstock, R. U., et al. (2015), Biodegradation: Updating the concepts of Control for microbial cleanup in contaminated aquifers, *Environ. Sci. Technol.*, *49*(12), 7073–7081, doi:10.1021/acs.est.5b00715.
- Mewafy, F. M., E. A. Atekwana, D. D. Werkema, L. D. Slater, D. Ntarlagiannis, A. Revil, M. Skold, and G. N. Delin (2011), Magnetic susceptibility as a proxy for investigating microbially mediated iron reduction, *Geophys. Res. Lett.*, *38*, L21402, doi:10.1029/2011GL049271.
- Murphy, F., and W. N. Herkelrath (1996), 1/1/13 1:23 PM A sample-freezing drive shoe for a wireline-piston core sampler, *Ground Water Monit. Remediat.*, *16*(3), 86–90.
- Naudet, V., and A. Revil (2005), A sandbox experiment to investigate bacteria-mediated redox processes on self-potential signals, *Geophys. Res. Lett.*, *32*, L11405, doi:10.1029/2005GL022735.
- Naudet, V., A. Revil, J.-Y. Bottero, and P. Bégassat (2003), Relationship between self-potential (SP) signals and redox conditions in contaminated groundwater, *Geophys. Res. Lett.*, *30*(21), 2091, doi:10.1029/2003GL018096.
- Naudet, V., A. Revil, E. Rizzo, J.-Y. Bottero, and P. Bégassat (2004), Groundwater redox conditions and conductivity in a contaminant plume from geoelectrical investigations, *Hydrol. Earth Syst. Sci.*, *8*(1), 8–22, doi:10.5194/hess-8-8-2004.
- Ntarlagiannis, D., E. A. Atekwana, E. A. Hill, and Y. Gorby (2007), Microbial nanowires: Is the subsurface “hardwired”?, *Geophys. Res. Lett.*, *34*, L17305, doi:10.1029/2007GL030426.
- Petiau, G. (2000), Second generation of lead-lead chloride electrodes for geophysical applications, *Pure Appl. Geophys.*, *157*(3), 357–382, doi:10.1007/s000240050004.
- Revil, A., C. A. Mendonca, E. A. Atekwana, B. Kulesa, S. S. Hubbard, and K. J. Bohlen (2010), Understanding biogeobatteries: Where geophysics meets microbiology, *J. Geophys. Res.*, *115*, G00g02, doi:10.1029/2009JG001065.
- Revil, A., P. Fernandez, D. Mao, H. K. French, E. Bloem, and A. Binley (2015), Self-potential monitoring of the enhanced biodegradation of an organic contaminant using a bioelectrochemical cell, *Lead. Edge*, *34*, 198–202, doi:10.1190/tle34020198.1.
- Risgaard-Petersen, N., L. R. Damgaard, A. Revil, and L. P. Nielsen (2014), Mapping electron sources and sinks in a marine biogeobattery, *J. Geophys. Res. Biogeosci.*, *119*, 1475–1486, doi:10.1002/2014JG002673.
- Risso, C., et al. (2009), Genome-scale comparison and constraint-based metabolic reconstruction of the facultative anaerobic Fe(III)-reducer *Rhodospirillum rubrum*, *BMC Genomics*, *10*(1), 447, doi:10.1186/1471-2164-10-447.
- Rotaru, A. E., P. M. Shrestha, F. Liu, B. Markovaite, S. Chen, K. P. Nevin, and D. R. Lovley (2014), Direct interspecies electron transfer between *Geobacter metallireducens* and *Methanosarcina barkeri*, *Appl. Environ. Microbiol.*, *80*(15), 4599–4605, doi:10.1128/AEM.00895-14.
- Sato, M., and H. M. Mooney (1960), The electrochemical mechanism of sulfide self-potentials, *Geophysics*, *25*(1), 226–249, doi:10.1190/1.1438689.
- Shrestha, P. M., A. E. Rotaru, Z. M. Summers, M. Shrestha, F. Liu, and D. R. Lovley (2013), Transcriptomic and genetic analysis of direct interspecies electron transfer, *Appl. Environ. Microbiol.*, *79*(7), 2397–2404, doi:10.1128/AEM.03837-12.
- Slater, L., A. Lund, E. A. Atekwana, S. Rossbach, D. Ntarlagiannis, and B. A. Bekins (2015), Indications of coupled carbon and iron cycling at a hydrocarbon-contaminated site from time-lapse magnetic susceptibility (MS) profiles, Abstract H41J-07 presented at 2015 Fall Meeting, AGU, San Francisco, Calif., 14–18 Dec.
- Xing, D., Y. Zuo, S. Cheng, J. M. Regan, and B. E. Logan (2008), Electricity generation by *Rhodopseudomonas palustris* DX-1, *Environ. Sci. Technol.*, *42*(11), 4146–4151, doi:10.1021/es800312v.
- Zachara, J. M., R. K. Kukkadapu, P. L. Gassman, A. Dohnalkova, J. K. Fredrickson, and T. Anderson (2004), Biogeochemical transformation of Fe minerals in a petroleum-contaminated aquifer, *Geochim. Cosmochim. Acta*, *68*(8), 1791–1805, doi:10.1016/j.gca.2003.09.022.
- Zhang, J., and Y. Lu (2016), Conductive Fe<sub>3</sub>O<sub>4</sub> Nanoparticles Accelerate Syntrophic Methane Production from Butyrate Oxidation in Two Different Lake Sediments, *Front. Microbiol.*, *7*, doi:10.3389/fmicb.2016.01316.
- Zhuang, L., J. Tang, Y. Wang, M. Hu, and S. Zhou (2015), Conductive iron oxide minerals accelerate syntrophic cooperation in methanogenic benzoate degradation, *J. Hazard. Mater.*, *293*, 37–45, doi:10.1016/j.jhazmat.2015.03.039.